Available online at www.sciencedirect.com
ScienceDirect
Earth and Planetary Science Letters 258 (2007) 359–377
EPSL
www.elsevier.com/locate/epsl

Miocene rotation of Sardinia: New paleomagnetic and geochronological constraints and geodynamic implications

J. Gattacceca [a,*], A. Deino [b], R. Rizzo [c], D.S. Jones [d], B. Henry [e], B. Beaudoin [f], F. Vadeboin [a]

[a] CEREGE, CNRS–Université Aix Marseille 3, BP 80, 13545 Aix-en-Provence Cedex 4, France
[b] Berkeley Geochronology Center, Berkeley, CA, 94530, USA
[c] Progetto CARG–Sardegna, Via Dolcetta 19, Cagliari, Italy
[d] Department of Earth and Planetary Sciences, Harvard University, 20 Oxford Street, Cambridge, MA 02138, USA
[e] Paléomagnétisme, IPGP, 94107 Saint-Maur-des-Fossés Cedex, France
[f] CGES, Ecole des Mines de Paris, 77305 Fontainebleau Cedex, France

Received 18 April 2006; received in revised form 29 January 2007; accepted 1 February 2007
Available online 11 February 2007
Editor: C.P. Jaupart

Abstract

The Miocene rotation of Sardinia (Western Mediterranean) remains poorly constrained despite a wealth of paleomagnetic data, primarily due to poor chronostratigraphic control. However, this rotation is contemporaneous with the opening of the Liguro-Provençal back-arc oceanic basin, and its history is key to understanding the kinematics of opening of the Western Mediterranean. We address this issue through paleomagnetic and $^{40}Ar/^{39}Ar$ geochronological investigations of Miocene volcanic sequences in Sardinia. Precise age control allows secular variation of the geomagnetic field to be evaluated. These data provide constraints on the rotational history of this continental microplate; Sardinia rotated 45° counterclockwise with respect to stable Europe after 20.5 Ma (Aquitanian), which is a marked increase over the estimate of 30° derived from prior paleomagnetic studies. Rotation was essentially complete by 15 Ma. About 30° of rotation occurred between 20.5 and 18 Ma (Burdigalian), corresponding to the period of maximum volcanic activity in Sardinia. The observed rotation validates palinspastic models derived from a morphological fit of basin margins, and indicates high rates of opening (up to 9 cm yr^{-1} in the southern part of the basin) between 20.5 and 18 Ma.

Keywords: paleomagnetism; Ar–Ar geochronology; Western Mediterranean; geodynamics; Sardinia; Liguro-Provençal basin

1. Introduction

A wealth of geological data (e.g. [1]) attests that the Corsica–Sardinia microplate (CSM) was proximal to the European continent before the opening of the Liguro-Provençal basin (Fig. 1). This basin is usually described as an Oligo–Miocene, partly oceanic, back-

* Corresponding author.
E-mail addresses: gattacceca@cerege.fr (J. Gattacceca), al@bgc.org (A. Deino), 927o9164@alice.it (R. Rizzo), dsjones@fas.harvard.edu (D.S. Jones), henry@ipgp.jussieu.fr (B. Henry), beaudoin@cges.ensmp.fr (B. Beaudoin), vadeboin@cerege.fr (F. Vadeboin).

0012-821X/$ - see front matter © 2007 Elsevier B.V. All rights reserved.
doi:10.1016/j.epsl.2007.02.003

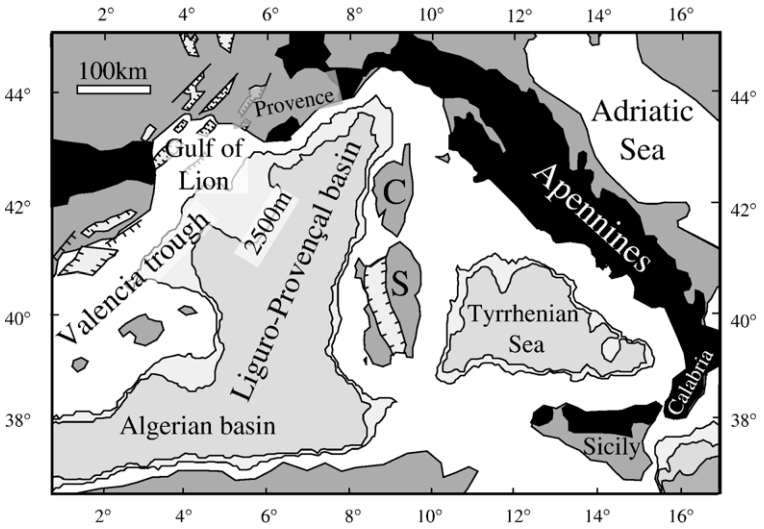

Fig. 1. Map of the western Mediterranean showing the Corsica–Sardinia block and surrounding ocean basins. Oligocene grabens and orogenic belts (dark grey) are outlined. Bathymetric contours: 2000, 2500 and 3000 m.

arc basin opening as a consequence of the eastward retreat and roll-back of an Adriatic/Ionian slab passively sinking into the mantle (e.g. [2,3]). Despite numerous geophysical studies, the original position of the CSM as well as the kinematics of the opening of the Liguro-Provençal basin remains controversial.

Several palinspastic reconstructions have been proposed for the CSM pre-drift (post-rift) location, based on differing geological and geophysical foundations ([4] for a review). Three groups of reconstructions can be identified (Fig. 2). The 'Model A' reconstruction was first proposed by Westphal et al. [5] based on a computer fit of 1000 m isobaths. A very similar reconstruction was later proposed based on morphological analysis of the basin margin [6,7]. 'Model B' was proposed by Burrus [8] with insight into the extent of the oceanic domain of the basin determined through seismic reflection data. 'Model C' was developed by Edel [9] based on paleomagnetic data from Sardinian Miocene volcanics and magnetic anomalies within the basin. Determination of the nature of the crust beneath a basin is often a useful tool in reconstructing its initial geometry. However, in the Liguro-Provençal basin, a variety of geophysical approaches have yielded contradictory results ([10–15], Online Fig. 1), due in particular to weak magnetic anomaly patterns within the basin [16].

Although the timing and geometry of rifting of the Liguro-Provençal basin is moderately well constrained between 30–28 Ma [17–19] and 21.5 Ma [18–20], the timing and geometry of the oceanic opening of the basin are poorly known. Oceanic spreading must have started slightly before or during late Aquitanian since late Aquitanian post-rift sediments are found in Sardinia [18] and in the Gulf of Lion [20] and mid-Aquitanian syn-rift sediments are found in Sardinia [18]. However, no data are available to constrain the termination of the oceanic spreading. The oceanic crust in the Liguro-

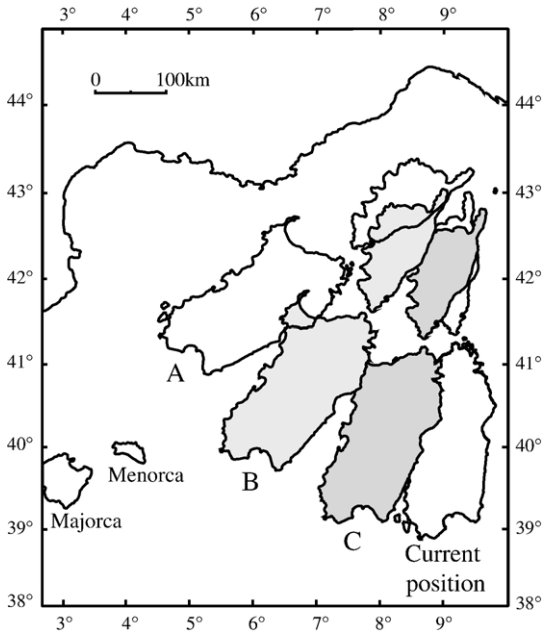

Fig. 2. Map of the Liguro-Provençal basin showing several reconstructions of the post-rift/pre-drift (~21.5 Ma) positions of Corsica and Sardinia, based on: (A) morphological fit of the continental margins of the basin (e.g. [7]); (B) determination of oceanic domain by seismic reflection [8]; (C) paleomagnetic data of Corsica–Sardinia and basin magnetic anomalies [9].

Provençal basin has not been drilled or sampled. Therefore the history of the opening of the Liguro-Provençal basin is best deduced from the record of CSM drift.

CSM drift was accompanied by a counterclockwise (ccw) rotation of the Corsica–Sardinia microplate with respect to stable Europe. Beginning in 1969 with De Jong et al. [21], this rotation has been investigated through paleomagnetic ([22,23] for a review) and geochronological ([24] for a review; [25]) studies in Sardinia but its timing has remained a matter of debate. An extensive paleomagnetic and K–Ar geochronological study of Sardinian volcanics allowed Montigny et al. [26] to propose a total 30° ccw rotation occurring rapidly between 21 and 19.5 Ma (ages recalculated in [27]). However, subsequent re-evaluation of the same data [22,23] appeared to demonstrate that the end of the rotation could not be constrained, due to the uncertainties in the paleomagnetic pole path introduced by secular variation of the geomagnetic field. Todesco and Vigliotti [22] attempted to resolve this issue by grouping the paleomagnetic directions obtained from Sardinian volcanic rocks on the basis of the regional stratigraphic framework [28]. However the ages of the stratigraphic units were ill-defined (Online Fig. 2), resulting in uncertainties whether dated units were interdigitated and actually span several Myr, or the existing K–Ar ages were unreliable. In addition, the absence of precise stratigraphic framework during paleomagnetic sampling led to oversampling of some volcanic units, thereby introducing bias in mean directions. Vigliotti and Langenheim [29] sought to solve the problem of secular variation recorded by the volcanics by focusing on Sardinian sediments, and demonstrated that rotation did not end before 16–15 Ma. Speranza et al. [30] showed a ~23° rotation of Sardinia after 19 Ma by examining the paleomagnetism of a well-dated sedimentary sequence. Edel et al. [31], from the paleomagnetism of a succession of five pyroclastic flows, proposed ~10° of rotation after 18 Ma. Vigliotti and Kent [32], from the paleomagnetism of Miocene sedimentary sequences of Corsica, concluded that rotation ended after ~15 Ma. This extensive pre-existing history of paleomagnetic and geochronological studies has demonstrated the difficulty of evaluating reliable rotation angles from volcanic rocks when the age control is not sufficiently precise to evaluate the importance of secular variation of the geomagnetic field. Another difficulty is that sedimentary rocks suitable for paleomagnetic studies are rare in Corsica and Sardinia [29,32,33]. We herein attempt to improve on these results by adding significant new data regarding the paleomagnetism and radiometric age of volcanic rocks from the Miocene of Sardinia. These new data permit us to critically evaluate proposed palinspastic reconstructions (Fig. 2).

2. Methods and techniques

2.1. Averaging paleosecular variation

At the latitude of Sardinia, the direction of the geomagnetic field is expected to vary 40–45° in declination and 25–30° in inclination at rates up to 10–15°/century, due to secular variation of the geomagnetic field [e.g. 34,35]. To obtain tectonic information from volcanic rocks, it is thus necessary to obtain directions from a number of different flows emplaced over an interval that is long with respect to secular variation (at least a few kyr) but short with respect to tectonic rotations (less than 1 Myr in the present case). Radiometric age constraints are thus a critical part of the tectonic reconstruction.

Previously, we presented paleomagnetic and $^{40}Ar/^{39}Ar$ geochronological results obtained from a 12-flow volcanic succession at Monte Furru in western Sardinia [27]. We demonstrated a ~13° ccw rotation after 18.1 Ma, confirming that the rotation of Sardinia ends later than proposed by Montigny et al. [26]. In this paper, to better constrain the Miocene rotational history of Sardinia, we present paleomagnetic and geochronological results from 8 additional Sardinian volcanic sequences (Fig. 3). Paleomagnetic sampling was preceded by a detailed stratigraphic study to avoid multiple sampling of single flows, and to constrain the age and the duration of emplacement of the succession with $^{40}Ar/^{39}Ar$ ages of key units.

2.2. Geochronology

Seventeen eruptive units (lava or pyroclastic flows, andesitic domes) were dated by the laser-heating, $^{40}Ar/^{39}Ar$ method. Plagioclase phenocryst separates (sanidine was unavailable) were prepared by way of grinding, sieving (400–800 μm), heavy liquid separation, magnetic separation, and hand-picking under a binocular microscope. Samples were irradiated on three occasions in the CLICIT facility of the Oregon State TRIGA reactor for periods from two to three hours. Sanidine from the Fish Canyon Tuff of Colorado was used as a neutron fluence monitor, with a reference age of 28.02 Ma [36]. Please note that using an alternative reference age for the Fish Canyon Tuff has only negligible effects on the absolute ages given in this paper and does not change the plate kinematics deduced from

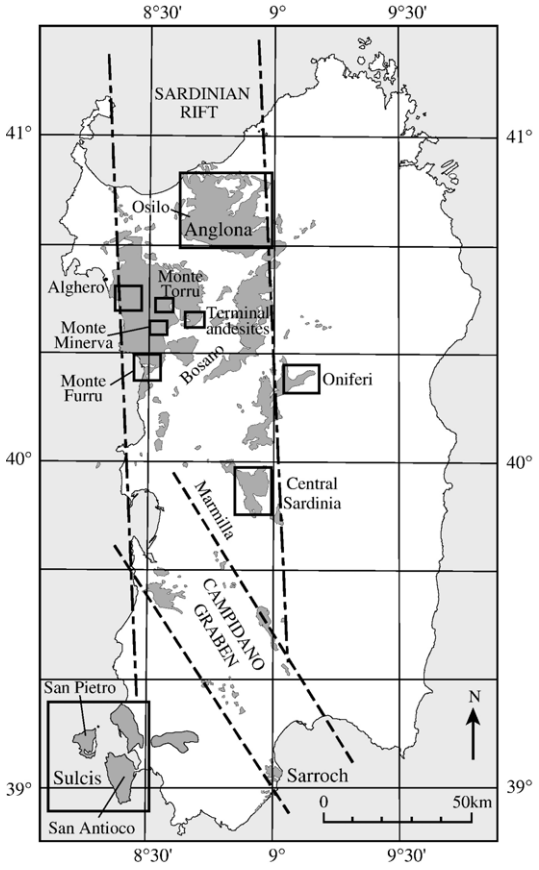

Fig. 3. Map of Sardinia showing location of Miocene calc-alkaline volcanism (shaded). Study areas are indicated by boxes.

these ages. After radiological cooling, samples were analyzed in a MAP-215 Noble gas mass spectrometer. Aliquots of about 50 mg of plagioclase were analyzed by the incremental-heating technique in nominally 15 steps using a square-profile, 6×6 mm CO_2 laser beam to heat the sample under ultra-high vacuum. Two aliquots were analyzed for most samples; in total, 30 incremental-heating experiments were performed. Results are summarized in Table 1.

The $^{40}Ar/^{39}Ar$ data can be internally evaluated for reliability based on the systematics of step-wise isotopic release for individual aliquots, aliquot-to-aliquot reproducibility, and conformance of the derived 'best' age to stratigraphic constraints. Representative step-wise argon release systematics are depicted in plots of apparent age versus cumulative percent ^{39}Ar release (Fig. 4). The plots for all samples are given in Online Fig. 3. Reproducibility of release patterns between replicate aliquots is generally quite good, though there is one notable exception (ONF); for this and other reasons this sample is considered problematic and will not be considered further in the geological interpretation of these data. Four samples out of the remaining 16 reveal rising spectra particularly in the latter phases of the experiments, and are interpreted to represent the trapping of excess $^{40}Ar^*$ reservoirs in small glass or fluid inclusions (e.g., dome A, Cuguruntis, Fig. 4a–b). Most other release patterns are flat or nearly so.

Apparent-age plateaus were identified in 16 of 30 experiments. 'Plateaus' as used herein are defined as comprising at least three contiguous steps encompassing more than 50% of the total ^{39}Ar, in which there is a 95% probability that the mean standard weighted deviation (MSWD) of the weighted-mean step ages can be attributed to analytical error alone. The search algorithm for a plateau also excludes steps wholly within the initial 10% of the ^{39}Ar release, since for this suite of plagioclase apparent ages for early release steps are often anomalously young, perhaps due to cryptic alteration. Thus they should not constitute part of any plateau sequence, which seeks to find the best eruptive age. All but one of the identified plateaus occurs within a broader sequence of similar ages. However, one occurs within a monotonically rising sequence (Monte Au, Fig. 4c) and probably provides a geologically less reliable age.

Integrated ages (calculated by mathematical isotopic recombination of the individual steps) are often not concordant with plateau ages but agreement improves dramatically when the first significant step (i.e., the first step with >2% of total ^{39}Ar release) is omitted from each incremental-heating experiment (MIS and MIH are good examples, Fig. 4e–f). Again, this is attributable to incipient alteration at or near crystal surfaces, along internal fractures, or from glass or mineral inclusions with release pathways to the crystal surface.

The best, geologically most accurate sample ages from these data are considered to occur where the apparent ages are virtually flat across most or all of the ^{39}Ar release (i.e., a plateau is found encompassing most of the spectrum), Ca/K ratios are stable, and the percentage of radiogenic $^{40}Ar^*$ of total ^{40}Ar ('$\%^{40}Ar^*$') is high. Replicate experiments should demonstrate similar release patterns and congruent ages. The two experiments from sample MIS illustrate data of this nature. Not all results in this data set are of such high quality; a few samples lack replicate experiments, some have more restricted plateaus, variable Ca/K ratios, or relatively low or irregular $\%^{40}Ar^*$. The quality of the individual experiments is discussed below on a case-by-case basis.

'Inverse isochron' correlation analyses ($^{36}Ar/^{40}Ar$ versus $^{39}Ar/^{40}Ar$) of plateau steps are provided in Table 1. The isochron analysis provides a test of the

Table 1
Summary $^{40}Ar/^{39}Ar$ analytical results

Sample	Run ID	Apparent age plateau					Integrated age			Isochron results				
		Age	*n*	MSWD	Prob.	% ^{39}Ar	Overall	Omitting 1st step (>2%)	%^{40}Ar*	Age	M.S.E.	($^{40}Ar/^{36}Ar)_{tr}$	M.S.E.	MSWD
		(Ma±1σ)					(Ma±1σ)	(Ma±1σ)						
Terminal andesites (isolated domes, not in stratigraphic order)														
Dome A	21965						15.1±0.2	15.41±0.08	79					
Dome A	21965b						15.4±0.2	15.54±0.09	74					
							15.25±0.14	**15.47±0.06**						
Cuguruntis	21966						15.6±0.2	15.69±0.13	62					
Cuguruntis	21966b						15.5±0.2	15.69±0.13	58					
							15.55±0.14	**15.69±0.09**						
Monte Au	21967						13.7±0.4	14.5±0.17	48					
Monte Au	21967b	14.92±0.08	8	1.2	0.31	51.5	15.2±0.6	15.3±0.2	43	**14.7**	**±0.2**	299.6	3.6	1.1
							14.16±0.33	14.84±0.13						
Monte Peidru	21968	15.45±0.06	6	1.1	0.33	50.1	15.1±0.2	15.23±0.09	71	**15.41**	**±0.1**	298.4	4.7	1.3
Monte Peidru	21968b						14.9±0.2	15.14±0.08	76					
							15.0±0.14	15.18±0.06						
Monte Minerva (top, base)														
MIS	21964	18.73±0.06	11	1.2	0.27	89.5	18.2±0.171	18.73±0.07	93	18.57	±0.08	330.7	13.9	0.6
MIS	21964b	18.81±0.06	8	0.5	0.86	75.0	18.37±0.2	18.75±0.08	88	18.72	±0.11	306.4	11.2	0.4
		18.77±0.04					18.28±0.13	18.74±0.05		**18.63**	**±0.07**			
MIH	21954	18.72±0.07	6	2.1	0.07	72.7	19.3±0.8	18.8±0.2	49	18.71	±0.11	296.0	3.4	2.6
MIH	21954b	18.78±0.07	6	2.1	0.06	72.2	19.0±0.4	18.7±0.12	69	19.14	±0.13	280.2	4.8	0.3
		18.75±0.05					19.06±0.36	18.73±0.1		**18.89**	**±0.08**			
Monte Torru– Monte Ruzzunis (top, base)														
MTB	21963						18.60±0.14	18.91±0.09	85					
MTB	21963b						18.62±0.17	18.99±0.1	80					
							18.61±0.11	**18.95±0.07**						
RUH	21955	18.90±0.06	12	0.9	0.59	92.6	18.58±0.13	18.89±0.08	87	**18.97**	**±0.09**	287.6	7.1	0.8
RUH	21955b						18.66±0.16	18.94±0.09	85					
							18.61±0.1	18.91±0.06						
Osilo andesites (Anglona)														
OSA	21980	18.87±0.06	9	1.5	0.17	66.1	18.3±0.2	18.81±0.08	86	**18.90**	**±0.07**	290.8	5.2	1.5
Oniferi area (top, intermediate, base)														
ONA	21979	20.41±0.07	6	1.5	0.19	64.1	20.17±0.09	20.3±0.09	89	**20.25**	**±0.13**	313.6	12.1	1.2
ONF	21981						4.89±0.02	4.89±0.02	82					
ONF	22251						44.14±0.18	45.04±0.19	96					
ONG	21977	20.75±0.06	6	0.9	0.45	57.5	20.19±0.08	20.53±0.08	96	**20.76**	**±0.07**	291.5	5.5	1.0
ONG	21977b						20.40±0.08	20.66±0.08	96					
							20.30±0.06	20.60±0.06						
Central Sardinia (top, intermediates, base)														
Ironi (IRO1)	22255						19.28±0.17	19.31±0.17	69					
Ironi (IRO1)	22255b	20.41±0.1	7	0.6	0.7	66.3	20.4±0.5	20.3±0.3	45	**20.40**	**±0.16**	295.9	3.0	0.7
							19.4±0.16	19.55±0.15						
Ruinas (RUI3)	21978	19.61±0.09	11	0.9	0.51	86.8	19.5±0.3	19.6±0.2	45	19.78	±0.17	292.5	2.6	1.0
Ruinas (RUI3)	22252	19.6±0.3	13	1.5	0.13	94.5	19.1±0.9	19.2±0.9	20	19.5	±0.69	296.0	3.0	1.0
		19.61±0.09					19.46±0.28	19.58±0.2		**19.76†**	**±0.16**			
Allai	21657	20.68±0.07	9	0.7	0.65	70.8	20.42±0.12	20.5±0.09	85	**20.91**	**±0.13**	266.2	14.2	0.3
Luzzana	21664						20.74±0.11	**20.94±0.09**	91					

(continued on next page)

Table 1 (*continued*)

Sample	Run ID	Apparent age plateau					Integrated age			Isochron results				
		Age	*n*	MSWD	Prob.	% ^{39}Ar	Overall	Omitting 1st step (>2%)	%^{40}Ar*	Age	M.S.E.	(^{40}Ar/^{36}Ar)$_{tr}$	M.S.E.	MSWD
		(Ma±1σ)					(Ma±1σ)	(Ma±1σ)						
Alghero area														
LGB	21976	20.68±0.06	8	1.1	0.36	78.1	20.63±0.08	20.67±0.08	97	20.65	±0.07	311.5	13.7	1.1
LGB	21976b	20.78±0.06	7	1.3	0.25	63.4	20.65±0.08	20.72±0.08	96	20.79	±0.08	288.0	19.3	1.6
		20.73±0.04					20.64±0.06	20.70±0.06		**20.71**	**±0.05**			

Best ages for each flow are in bold (see text). † indicates an age that is apparently too young (see text). *n*: number of steps in the plateau; MSWD: mean sum of weighted deviates calculated for the plateau steps; Prob: probability that the MSWD is due to analytical scatter alone; %^{39}Ar: percentage of ^{39}Ar in the plateau versus the total ^{39}Ar released across all steps; 'Omitting first step >2% total ^{39}Ar': integrated age calculated omitting the first step with greater than 2% of the total ^{39}Ar; '%^{40}Ar*': percentage of radiogenic argon in the sum of the atmospheric and radiogenic ^{40}Ar released; M.S.E. is the 'modified standard error,' where if the MSWD is >1, then the standard error is multiplied by root MSWD. Full analytical data for isotopic interference parameters, isotopic constants, and decay rates are provided in Online Table 1.

composition of the 'trapped' argon component, which nominally should be atmospheric with a ^{40}Ar/^{36}Ar ratio of 295.5. Of the 16 plateaus detected, all but three have (^{40}Ar/^{36}Ar)$_{tr}$ indistinguishable from the expected atmospheric ratio. Two of these exhibit compositions that are slightly subatmospheric ('trapped' component less than atmospheric ratio), and one that is slightly superatmospheric; these are barely statistically significant at the 95% confidence level and may not truly reflect geological compositions. ^{40}Ar/^{39}Ar ages derived from the isochrons are all indistinguishable from the plateau ages at the 95% confidence level. The isochron ages are preferred over the conventional plateau ages, as the isochron analysis inherently accommodates departure from the rigid assumption that (^{40}Ar/^{36}Ar)$_{tr}$ must equal that of the present atmosphere.

Conformance to internal stratigraphic constraints is a further indicator of geological accuracy and reliability. As shown below, the ^{40}Ar/^{39}Ar ages are in agreement with the observed stratigraphy with the exception of a single flow in central Sardinia.

2.3. Paleomagnetism and interpretation of paleomagnetic data

A total of 118 sites were studied in eight Sardinian volcanic areas (Fig. 3). Samples were obtained *in situ* using a portable, gasoline-powered drill. Cores were oriented with solar and magnetic compass. The magnetic mineralogy was studied by means of isothermal remanent magnetization acquisition, hysteresis loops, and thermomagnetic analyses performed with a CS2 apparatus. The anisotropy of magnetic susceptibility was measured with KLY2 and KLY3 kappabridges to identify samples with strong petrofabric. Paleomagnetic analyses were conducted at IPGP (Saint-Maur, France), INGV (Rome, Italy) and CEREGE (Aix-en-Provence, France). The natural remanent magnetizations were measured with JR4 or JR5 Agico spinner magnetometers (IPGP, CEREGE) or 2G cryogenic magnetometers equipped with DC SQUIDs (INGV, CEREGE). Alternating field and thermal stepwise demagnetizations were used. Demagnetization data were evaluated using principal component analyses [37]. A few sites, in particular those struck by lighting, required the use of the remagnetization circles method. Fisher's [38] statistics were used to calculate mean directions. All paleomagnetic data have been processed using Paleomac software [39]. Representative demagnetization data are plotted on Fig. 5. The main magnetic carrier is (titano-)magnetite, as demonstrated by magnetic saturation below 300 mT (Online Fig. 4a) and Curie temperatures between 530 and 580 °C. Maghemite is sometimes present but bears the same paleomagnetic directions as magnetite. Hysteresis loops indicate pseudo-single-domain grains in most cases, and multidomain grains in some andesites (Online Fig. 4b). The degrees of anisotropy of magnetic susceptibility (ratio of maximum to minimum susceptibility) are generally below 1.03, some exceptions being discussed below. Magnetic properties of the studied volcanics (NRM, susceptibility, Curie temperature, hysteresis parameters, anisotropy degree) are detailed in Online Table 2. The paleomagnetic results are shown in Table 2. A synthesis of the paleomagnetic and geochronological results for each area is shown in Table 3.

Paleomagnetic results were interpreted on a succession-by-succession basis. First, transitional paleomagnetic directions were discarded using Vandamme's [40] recursive method. Successive volcanic flows within a pile sometimes provide indistinguishable paleomagnetic directions indicating that these flows were probably emplaced within a time frame that is short with respect to secular variation, i.e. a few centuries at most. If field

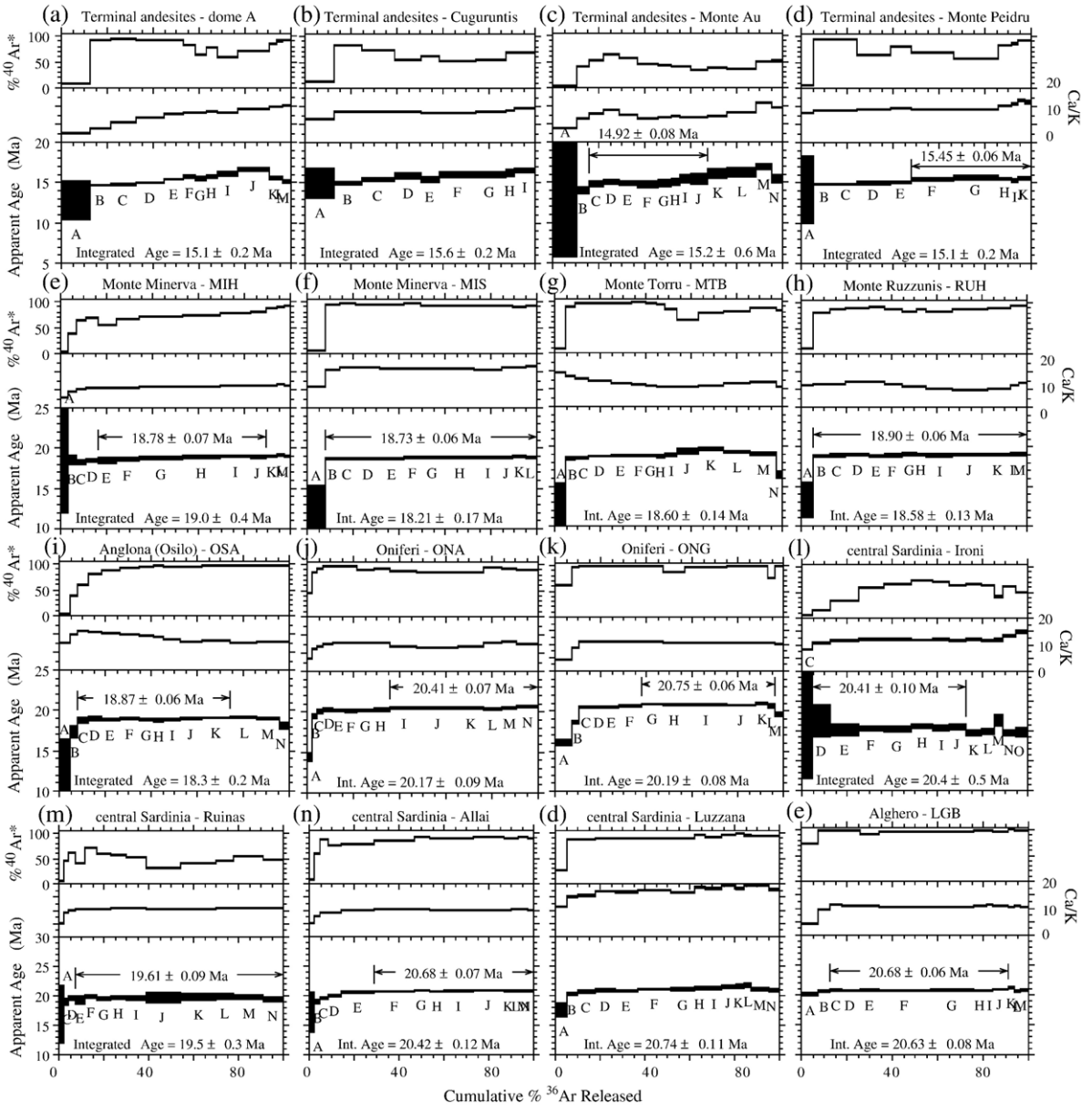

Fig. 4. Apparent age versus percent of total ^{39}Ar released for the ^{40}Ar/^{39}Ar incremental-heating experiments on plagioclase from Sardinian volcanic rocks. Auxiliary plots of Ca/K ratio and the percentage of radiogenic ^{40}Ar of total argon are also shown against the same horizontal axis.

evidence, such as the absence of paleosols, supported this interpretation, we used the statistical approach of McElhinny et al. [41] to confirm that these successive flows had not recorded independent magnetic field directions. The directions given by these flows are then averaged and treated as a single paleomagnetic direction. Next a mean paleomagnetic direction for the entire succession was computed and compared to that derived from the coeval paleomagnetic pole for stable Eurasia: 84.2°N, 154.9°E, A_{95}=3.2 at 15 Ma and 81.4°N, 149.7°E, A_{95}=4.5 at 20 Ma [42]. The 95% confidence limits on rotation and flattening were computed according to Demarest [43].

Finally, the angular standard deviation of the VGPs around the mean VGP (δ) is calculated after rejection of transitional VGPs. This parameter provides a useful index for the extent of incorporation of secular variation, and can be compared to values derived from paleomagnetic databases that suggest, at the latitude of Sardinia for the interval 0–5 Ma, 15°<δ<17° [44]. A volcanic

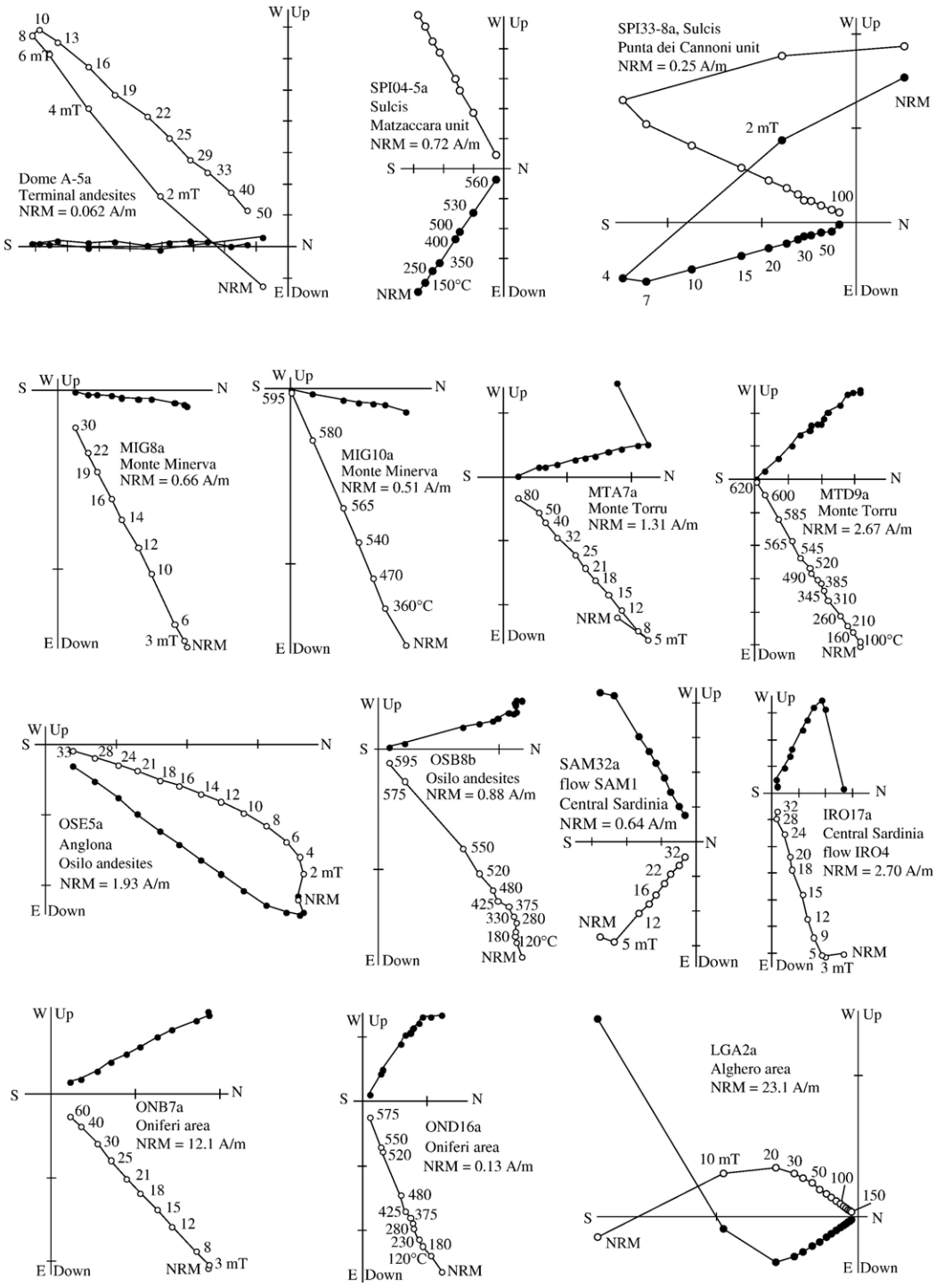

Fig. 5. Orthogonal projection plots of stepwise demagnetization data of representative samples. At least one sample is shown for each study area. Open and solid symbols represent projections on vertical and horizontal planes, respectively.

succession displaying a significantly lower δ has probably not thoroughly averaged secular variation, hence may not provide reliable tectonic information. As Sardinia did not significantly move latitudinally during the Miocene, the comparison of the succession mean inclination with the expected lower Miocene inclination

Table 2
Paleomagnetic results

Site	$D°$	$I°$	$\alpha_{95}°$	k	n/n_0	Ref.
Terminal andesites						
Monte Larenta**	159	−40	19	42	3/3	[48]
Monte Larenta	160	−59	3	594	6/6	[9]
Monte Mundigu**	159	−40	18.5	45	3/3	[49]
Monte Mundigu	9	58	4.9	130	8/8	
Castello di Bonvei**	177	−11	58	5	3/3	[48]
Castello di Bonvei**	196	−43	31.5	16	3/3	[49]
Castello di Bonvei	212	−36	6.3	82	8/9	
Monte Ozzastru	165	−14	10.5	142	3/3	[49]
Monte Peidru	184	−65	2	1603	4/4	
Monte Au	178	−48	4	367	5/5	
Dome A	178	−43	3.7	451	4/4	
Dome B	180	−35	12.8	39	4/5	
Cuguruntis	186	−30	7.7	186	5/5	
Ozzastru**	–	–	–	–	0/4	
Monte Pizzinu**	–	–	–	–	0/7	
Sulcis area						
Geniò (16?)	189	−71	1.4	2054	7/7	
Punta Mingosa (15)	357	36	2.9	426	7/7	
12** (Punta Mingosa)	0	45	4.6	400	4	[56]
Serra Paringianu1 (14)	182	−20	8.5	51	7/7	
Serra Paringianu2 (14)	166	−3	3.3	240	9/9	
11** (Serra Paringianu2)	150	−7	26.6	13	4	[56]
13** (Serra Paringianu2)	147	−6	27.4	21	3	[56]
Paringianu (13)	209	−28	4.2	82	15/15	
Monte Ulmus (12)	179	−45	2.6	89	34/36	
14** (Monte Ulmus)	175	−50	18.9	25	4	[56]
Comendite1 (11)	196	−60	2.4	133	27/29	
Comendite2 (10)	17	43	4.5	152	8/8	
Comendite3 (9)	16	50	4.0	188	8/8	
Comendite4 (9)	20	60	5.5	129	8/8	
Comendite5 (9)	338	52	5	235	5/5	
Matzaccara (8)	130	−47	2.1	1020	6/7	
Punta dei Cannoni (7)	162	−45	8.8	61	6/6	
Nuraxi (6)	163	−15	2.2	115	36/36	
10** (Nuraxi)	165	−22	17.7	50	3	[56]
Conca Is Angius** (5)	177	−24	3.7	473	5/6	
Monte Crobu** (4)	164	64	3.6	116	15/15	
Seruci** (3)	11	34	2.4	336	12/14	
Acqua Sa Canna** (2)	356	60	4.4	193	7/8	
Lenzu** (1)	19	58	6.4	143	5/6	
Monte Minerva						
SI2-II‡ (12)	358	36	7	315	3/3	[49]
MIA‡ (12)	6	32	–	–	10/11	
MIS‡ (11)	4	36	2.6	455	8/8	
MIB# (10)	342	50	4.1	219	6/6	
MIC# (9)	338	50	1.9	851	8/8	
MID‡ (8)	346	55	3.5	215	8/10	
MIE‡ (7)	346	51	6.5	150	8/7	
MIF3 (6)	355	58	4.8	196	6/6	[57]
MIF2# (5)	351	55	2.9	316	9/9	[57]
MIF1# (4)	350	52	3.9	114	13/13	[57]
MIF0# (3)	352	51	2.1	1915	4/4	[57]
MIG (2)	6	63	2	768	8/8	
MIH (1)	357	50	5	150	6/7	
Monte Torru/Monte Ruzzunis						
SI2-I (9)	356	38	12	32	6/6	[49]
148 (9)	341	53	2	2089	4/4	[9]
Monte Torru/Monte Ruzzunis						
RUA, MTA (9)	343	54			10/10	
RUB, **MTB** (8)	339	57	2	705	8/8	
RUC, MTC‡ (7)	325	48	1.9	412	14/14	
RUD, MTD‡ (6)	326	49	2.2	409	11/13	
RUE, MTE (5)	325	43	2.1	270	19/19	
RUF, MTF# (4)	332	48	3.4	186	10/10	
RUX# (3)	326	48	2	817	7/9	
RUG# (2)	332	50	2.7	510	6/6	
RUH# (1)	329	50	3.2	300	7/7	
133** (?)	328	48	1.0	8000	4/4	[9]
Osilo andesites (Anglona)						
BON** (8)	–	–	–	–	0/10	
OSD (7)	346	51	1.7	915	9/10	
OSE‡* (6)	31	18	8.0	49	8/8	
OSF‡* (5)	22	12	6.5	74	8/8	
OSC* (4)	36	8	8.9	40	8/8	
OSI# (3)	351	56	4.2	262	6/6	
OSB# (2)	345	53	4.5	114	10/10	
116# (2)	343	53	3	465	6/7	[9]
OSA (1)	355	48	2.6	669	6/7	
Central Sardinia						
IRO4 (12)	303	60	7.5	113	4/4	
IRO3 (11)	157	−42	3.8	261	6/6	
IRO2 (10)	164	−38	2.8	700	5/5	
IRO1 (9)	136	−52	3.2	451	5/6	
RUI3 (8)	112	−52	3.7	346	5/5	
RUI2 (7)	103	−64	4.2	271	5/5	
RUI1 (6)	126	−64	6.3		7/7	
SAM3 (5)	290	64	4	643	3/3	
SAM2 (4)	290	42	8.8	83	4/4	
SAM1 (3)	337	13	3.4	148	12/12	
Allai (2)	132	−56	5.7	46	15/15	
Luzzana (1)	129	−24	5.7	72	9/11	
Oniferi area						
ONA2 (10)	132	−40	1.9	1277	5/5	
ONA1 (9)	339	5	1.2	6503	3/3	
ONB (8)	330	51	4.9	132	7/7	
ONC (7)	324	64	3	414	6/6	
OND2 (6)	294	62	3.1	487	5/6	
OND1 (5)	127	−35	3	309	7/7	
ONE2# (4)	354	58	2	1586	4/4	
ONE1# (3)	351	56	3.4	534	4/4	
ONF (2)	321	65	3.5	312	6/6	
ONG (1)	150	−62	3.4	416	5/5	
Alghero area						
10	283	49	4	219	7/7	[21]
9	284	55	8	97	5/5	[21]
8	139	−43	9	48	7/7	[21]
7	146	−28	2.5	1090	5/5	[21]
6 (10)	163	−43	3	990	4/5	[21]
LGH (9)	134	−51	2.9	427	7/7	
5 (8)	153	−40	4	415	5/5	[21]
LGG (7)	349	12	3.2	235	10/10	
4 (6)	341	16	1.5	1090	11/11	[21]
3 (5)	325	43	6	137	6/6	[21]
2 (4)	317	43	6.5	144	5/5	[21]
LGB (3)	145	−55	4.8	160	7/8	

(continued on next page)

Table 2 (*continued*)

Site	$D°$	$I°$	$\alpha_{95}°$	k	n/n_0	Ref.
Alghero area						
LGA (2)	144	−31	2.2	480	10/10	
1 (1)	148	−47	4.5	386	4/5	[21]

D and I are mean declination and inclination. α_{95} and k are Fisher's statistical parameters [38]. n/n_0, number of samples used to calculate the mean direction/total number of measured samples.
When available, stratigraphic order within the succession is indicated in parentheses after site names. # or ‡ indicates indistinguishable directions from successive flows that were averaged as a single direction before computing a mean direction for the succession. *Transitional direction according to Vandamme's criteria [40]. **Other sites not considered for computation of the mean direction (see text). Sites indicated in bold were dated by the $^{40}Ar/^{39}Ar$ method. For the Sulcis and Central Sardinia areas, several pyroclastic flows were sampled at more than one locality and provided indistinguishable directions which were averaged and treated as single paleomagnetic directions (see Online Figs. 6a–b and 8). Precise geographic location of the sampling sites can be found on the maps provided as supplementary figures (terminal andesites: Online Fig. 5; Sulcis: Online Fig. 6a and b; Osilo andesites: Online Fig. 7; central Sardinia: Online Fig. 8; Oniferi area: Online Fig. 9; Alghero area: Online Fig. 10).

(~55°) also gives a means of judging of whether secular variation has been completely averaged.

All the correlations with the magnetostratigraphic scale are made according to the timescale of Lourens et al. [45].

3. Results

3.1. Terminal andesites

The 'Terminal Andesites' (SA3 in the stratigraphic scheme of Coulon [28]) represent the most recent calc-alkaline volcanism in Sardinia, and consist of about 30 andesitic units (domes and dikes) spread over an area of 20 km^2 (Online Fig. 5). Horizontal middle Miocene sediments onlap the volcanic structures [46]. Previous K–Ar ages [26,47] are problematic as they yield an improbable wide age span for such a small field, from 13.1 to 18.1 Ma, and provide inconsistent ages for individual domes. For example, the Monte Larenta dome is dated at 13.14±0.2 and 13.47±0.2 Ma by K–Ar on whole rock [47], and 17.1±0.8 and 18.1±1.1 Ma by K–Ar on plagioclase [26].

Six paleomagnetic sites were previously studied in this area ([9,48,49], Table 2). Most of these reverse-polarity directions are poorly defined. We rejected all directions with $\alpha_{95}>15°$. Therefore, only the directions from Monte Larenta [9] and Monte Ozzastru [49] are considered further.

We studied nine paleomagnetic sites in this area (Online Fig. 5). For several domes, demagnetization yielded two components of magnetization (Fig. 3, sample "Dome A"). The high-coercivity/high-temperature component was interpreted as primary magnetization. The Monte Pizzinu site was completely remagnetized by lighting strikes. Four domes were sampled for $^{40}Ar/^{39}Ar$ dating and two reliable ages were obtained: 14.7±0.2 and 15.41±0.10 Ma (1σ analytical error). The geochemical similarities of the domes [47], the reverse polarity of all paleomagnetic directions but one, and the narrow span of the $^{40}Ar/^{39}Ar$ chronology suggest that the entire dome complex may have formed during a relatively short interval possibly between chrons 5Bn.2r and 5ADr. Scatter of paleomagnetic directions is adequate ($\delta=18.5°$). The mean

Table 3
Synthesis of paleomagnetic and geochronological results

Volcanic succession	$D°$	$I°$	$\alpha_{95}°$	k	N	$\delta°$	$R°$	$F°$	Age (Ma)
Terminal andesites	1.5	44.0	12.7	17	9	18.5 (14.0–27.4)	**2.5**±14.6	11.1±10.5	14.7–15.4
Sulcis area	357.9	43.0	12.3	11	14	23.8 (19.0–31.8)	5.9±13.9	10.7±10.2	15.1–15.8
Monte Furru	351.1	52.9	7.3	51	8	11.6 (8.8–17.1)	**15.3**±10.6	−0.2±7.0	18.1–18.2
Monte Minerva	354.3	52.0	8.1	56	7	11.3 (8.4–17.2)	12.2±11.4	1.0±7.5	18.6–18.9
Monte Torru	331.8	50.2	7.2	91	5	8.6 (6.2–14.2)	34.7±10.0	2.9±6.9	18.6–19.0
Osilo andesites	10.8	37.3	28.8	8	5	26.1 (18.2–45.8)	−4.3±30.1	16.1±23.3	~18.9
Minerva/Torru/Osilo	345.7	51.7	5.0	60	15	12.4 (9.9–16.6)	**20.8**±7.8	1.5±5.5	18.6–19.0
Central Sardinia	313.1	49.4	11.8	15	12	21.9 (17.1–30.5)	53.4±15.3	3.1±10.2	20–20.9
Oniferi	323.7	50.4	14.6	13	9	20.8 (15.7–30.8)	42.8±19.1	2.5±12.3	20.3–20.8
Alghero	324.4	41.1	9.7	18	14	19.5 (15.5–26.4)	42.1±11.2	11.9±8.6	20.2–20.8
Alghero/Oniferi/Central	320.6	46.4	6.4	15	35	21.1 (18.1–25.3)	**45.9**±8.6	6.4±6.4	20–20.9

D, I: mean declination and inclination for the volcanic succession; α_{95}, k: Fisher statistics parameters [38]; N: number of independent directions used for the mean; δ: angular standard deviation of the VGPs around their mean after rejection of transitional VGPs (with upper and lower limits of the 95% confidence interval calculated after [78]); R, F: rotation and flattening with respect to the direction computed from stable Eurasia paleomagnetic pole [41]. Rotation and flattening for Monte Furru are recomputed after [27]. Successions or grouped successions in bold characters provide the tectonic rotations used in the discussion.

paleomagnetic direction suggests weak or absent rotation (Table 3).

3.2. Sulcis area

Southwestern Sardinia, separated from the rest of Sardinia by the Pliocene–Quaternary Campidano graben, displays abundant Miocene calc-alkaline volcanism (Sulcis and Sarroch areas, Fig. 3). About 20 sites were studied in the Sarroch area [50,51] and provided W declinations that indicate about 90° of ccw rotation during the Miocene. However, the sites are distributed along the southwestern border of the Campidano graben and the observed rotations were attributed to local tectonics [51]. Miocene volcanism in the Sulcis area is represented by an accumulation of up to 500 m of volcanic materials, mainly extensive pyroclastic flows well exposed on San Pietro and San Antioco islands, and on the mainland near Carbonia. The stratigraphy of the pyroclastic volcanism is known thanks to industrial boreholes [52,53]. The stratigraphy of the studied succession is given in Table 2. The Serra di Paringianu formation, close to the top of the succession has a $^{40}Ar/^{39}Ar$ age of 15.1±0.2 Ma [54]. The Nuraxi formation has a $^{40}Ar/^{39}Ar$ age of 15.79±0.16 Ma [79]. For base of the studied succession, only whole rock K/Ar (16.6±0.8 Ma for the Acqua sa Canna formation) and Rb/Sr (16.5±0.9 Ma for the Lenzu formation) ages are available [55]. Six paleomagnetic sites had been previously studied in this area [9,56] but their stratigraphic position was unclear and the data too limited to allow robust interpretation. We have studied the paleomagnetism of 33 sites in the pyroclastic succession beginning with the Lenzu formation through the top of the succession on San Pietro Island (see Online Fig. 6a–b for sampling maps). Some flows were sampled at several sites and provided indistinguishable directions which were averaged and treated as single paleomagnetic directions. The Miocene volcanics are cut by vertical faults. In this type of pyroclastic succession, it is sometimes difficult to distinguish between initial depositional dip and tectonic deformation, thus a tilt correction was not applied to the paleomagnetic data. In any event, the maximum observed tilt is less than 10° so that corrections would be minor and would mostly affect the paleomagnetic inclination. The five paleomagnetic directions from Manzoni [56] compare well with our data and can be ascribed to specific volcanic flows (Table 2), but we choose to utilize only our own data since Manzoni's directions are obtained by blanket treatment at 50 mT and have larger α_{95}. We obtained 19 independent paleomagnetic directions (Table 2). In view of the lack of reliable ages for the bottom of the studied succession, we considered only the directions obtained from the top of the succession down to the Nuraxi formation. The scatter of these 14 paleomagnetic directions is satisfactory (δ=24°). The mean direction suggests little or no rotation (Table 3). The slight inclination flattening may be attributed to the absence of tilt correction and/or remanence anisotropy in welded pyroclastic flows.

3.3. Monte Minerva and Monte Torru successions

Monte Minerva (40°27′38″N, 8°32′28″E) exposes a flat-lying, 300 m thick succession of poorly to strongly welded pyroclastic flows on its northern flank. We sampled 12 flows for paleomagnetism (Table 2). Anisotropy of magnetic susceptibility is low for most flows but up to 8% for the most welded units (MIF0, MIF1). Remanence anisotropy measurements demonstrated that magnetic anisotropy was responsible for an inclination shallowing of 8 and 6° for MIF0 and MIF1 respectively [57]. One paleomagnetic site had been previously studied in the top flow of the succession (site SI2-II [49]), like our site MIA. Both sites provide indistinguishable paleomagnetic directions. All studied flows have normal paleomagnetic polarity suggesting emplacement within a single normal polarity interval, an inference also supported by the absence of interflow paleosols. The weighted mean of new replicate $^{40}Ar/^{39}Ar$ ages are 18.63±0.07 and 18.89±0.08 for the top and base of the succession, respectively. These results suggest rapid accumulation, within a few hundred thousand years, of the Monte Minerva succession during chron 6n. Several groups of successive flows provided indistinguishable paleomagnetic directions and were averaged and treated as a single paleomagnetic direction. In view of the small number of independent directions (7) and their low scatter (δ=11°), the inferred 12±11° ccw rotation remains qualitative.

The Monte Torru pyroclastic succession was studied at two localities 3 km apart, at Monte Torru (40°33′10″N, 8°37′23″E) and Monte Ruzzunis (40°32′50″N, 8°35′38″E). Nine pyroclastic flows were distinguished along the 200 m thick succession and correlated between sections. Whenever possible, the flows were sampled for paleomagnetism at both localities. The paleomagnetic directions (corrected for a 5°S tectonic tilt) are identical for the same flows from the two sections, confirming that the dispersion observed between the different flows is not due to sampling problems or local magnetic effects. Therefore, the directions

for the same flow from the Monte Torru and Monte Ruzzunis sections have been averaged and treated as single paleomagnetic directions. Three paleomagnetic sites had been previously studied (Table 2), two of them on the top flow (SI2-I, 148), the third (133) being difficult to locate in the stratigraphic sequence. The 3 directions from the top flow (sites SI2-I, 148 and our site RUA) were averaged and treated as a single paleomagnetic direction. After combining successive indistinguishable directions, only five independent directions are left. The absence of polarity reversals and of intervening paleosols suggest relatively rapid emplacement of the entire sequence. The top flow was previously dated by K–Ar at 16.21±1 Ma (whole rock [47]). Site 133 was dated at 19.1±0.5 and 17.6±0.1 Ma (K–Ar on biotite and plagioclase respectively [26]). These three determinations fail to provide useful constraints on the age of emplacement and duration of the succession. Two aliquots of sample RUH from the base of the sequence yielded similar argon release patterns, though only one experiment yielded a plateau by the defined criterion, for an isochron age of 18.97±0.09. This is considered to be a geologically reliable result, due to the flatness of both spectra, the high percentage radiogenic ^{40}Ar content throughout (%^{40}Ar*), and the reproducible integrated ages (18.58, 18.66 Ma). However, a sample from the top of the succession (MTB) exhibited release spectra that climbed by ~1 Ma during the course of experiments on two aliquots, and so a precise eruptive age could not be determined. Nevertheless the reproducibility of integrated ages (18.60±0.14 and 18.62±0.17 Ma), conformance to stratigraphic relationship, and similarity to the age of RUH suggests that the integrated ages are approximately correct. The geochronologic evidence indicates that the succession was emplaced beginning about 19 Ma, and all indications support accumulation of the succession within chron 6n. In view of the small number of independent directions (5) and their very low scatter (δ=8.6°), the inferred 35±10° ccw rotation appears unreliable.

3.4. Anglona

Numerous paleomagnetic studies, encompassing more than 60 sites, have been performed in the Anglona area ([22] for a synthesis). However, stratigraphy of the area is poorly known due to poor outcrop, so interpretation of the paleomagnetic data remains problematic. A schematic stratigraphy is provided ([28], Online Fig. 2). Lower units (andesites, lower lacustrine sediments and intercalated volcanics) have more westerly mean declinations than upper units [22] but no quantitative information can be derived from the existing data.

We studied eight sites distributed vertically in a 300 m thick succession of andesitic lavas near the town of Osilo (40°44′36″N, 8°40′18″E, see Online Fig. 7 for a sampling map). The section has experienced epithermal alteration and calcite mineralization. Three directions from successive lower sites record a peculiar geomagnetic direction with a very low inclination (sites OSC, OSF, OSE) but are not rejected by Vandamme's recursive method [40]. The uppermost site did not provide a reliable paleomagnetic direction probably because of lighting strikes. Successive flows OSB (equivalent to site 16 of Edel [9]) and OSI have indistinguishable paleomagnetic directions. The same applies for successive flows OSF and OSE. Therefore we record only five independent paleomagnetic directions, which is too small to compute a reliable tectonic rotation. We obtained an excellent plateau with high %^{40}Ar* yields from a plagioclase separate from one flow (OSA), yielding a ^{40}Ar/^{39}Ar isochron age of 18.90±0.07 Ma. The normal polarity of all the paleomagnetic directions suggests that the succession was emplaced within chron 6n.

3.5. Central Sardinia

We investigated 16 sites in Central Sardinia (39°55′N, 8°55′E) in a 200 m thick volcano-sedimentary succession composed of five pyroclastic units separated by continental fluvio-deltaic sediments (Fig. 6, [58]). Some flows were sampled at several sites and provided indistinguishable directions which were averaged and treated as single paleomagnetic directions. A sampling map is provided in Online Fig. 8. No previous paleomagnetic data were available for this succession. The two lower units are within a single pyroclastic flow, whereas the upper three consist of individual flows. The succession lies directly on Paleozoic basement. Despite strong anisotropy of magnetic susceptibility for some sites (IRO2 for instance), no inclination shallowing was detected [57].

A K–Ar age of 20.8±1 Ma was previously obtained on one flow of Monte Ironi unit near site RUI3 [24]. We acquired ^{40}Ar/^{39}Ar ages on four of the five units. Best ages from bottom to top are: 20.74±0.11 (Luzzana, integrated age, no plateau obtained); 20.91±0.13 Ma (Allai; single plateau); 19.76±0.16 Ma (Ruinas at RUI3 site; two plateaus); and 20.40±0.16 Ma (Ironi at IRO1 site; one plateau from two experiments). The age for the Ironi flow is too old compared to the underlying Ruinas unit. Results from both samples are compromised

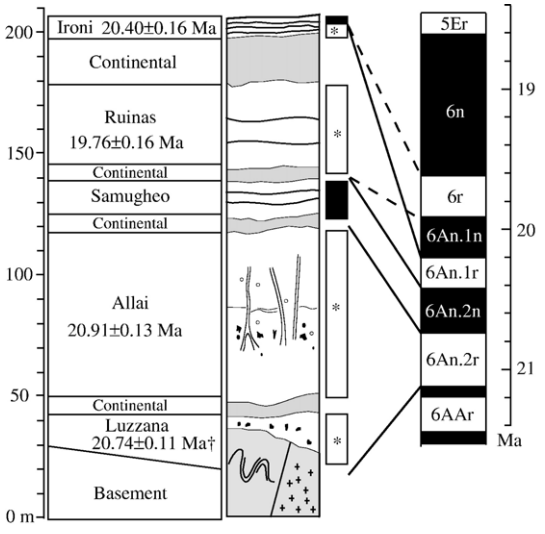

Fig. 6. Schematic log of the Central Sardinia succession (after [58]) with $^{40}Ar/^{39}Ar$ geochronological ages and paleomagnetic polarity. Asterisks indicate the stratigraphic positions of dated flows. Two different correlations with the reference magnetostratigraphic scale [44] are proposed for the upper part of the succession according to whether the age for Ironi (solid lines) or Ruinas (dashed lines) is considered reliable. †The age for Luzzana is an integrated age (no plateau, see text).

by relatively low radiogenic content and a lack of demonstrated reproducibility; the contradiction in radiometric age relationships cannot be explained by the $^{40}Ar/^{39}Ar$ systematics alone. If the age for Ironi is correct, the Ruinas and most of the Ironi units were likely emplaced during chron 6An.1r, and flow IRO4 (the only normal polarity flow Ironi unit) may represent the base of chron 6An.1n (Fig. 6). In this scenario, the central Sardinia volcanic succession would lie constrained between 20.9 and 20.2 Ma. If the age for Ruinas is correct, the Ruinas and Ironi units were likely emplaced during chron C6r, and flow IRO4 may represent the base of chron 6n (Fig. 6). In this scenario, the central Sardinia volcanic succession would be constrained between 20.9 and 19.8 Ma. In both cases, the emplacement of the succession is rapid with respect to tectonic movements, and thus a calculation of mean paleomagnetic direction should essentially average secular variation. The mean direction based on 12 independent directions yields a 53.4°±15.3° ccw rotation, with δ=21.9° indicating adequate averaging of secular variation.

3.6. Oniferi area

This area (40°18′N, 9°11′E) contains at least ten pyroclastic flows lying directly on the Paleozoic basement. Neither paleomagnetic nor geochronological data were previously available for the area. Ten sites were sampled for paleomagnetism (Online Fig. 9). Reverse and normal polarity directions were evidenced but the lack of detailed stratigraphy within the succession prevents correlation with the magnetostratigraphic timescale. We obtained $^{40}Ar/^{39}Ar$ isochron ages from plateaus from the base (20.76±0.07 Ma) and the top (20.25±0.13 Ma) of the succession. Although the plateaus for the older unit (ONG) are not as broad as found in some experiments, the integrated ages are fairly reproducible, the relatively flat portion beyond the strict plateau is broad, Ca/K ratios are stable, and $\%^{40}Ar^*$ is very high (near 100%), all suggesting reliable geochronometry. The characteristics of the $^{40}Ar/^{39}Ar$ incremental heating results for the upper sample are very similar and judged reliable, yielding a duration for the succession of about 500 kyr. The mean direction based on 9 independent directions yields a 42.1± 11.2° ccw rotation, with δ=19.5° indicating adequate averaging of secular variation.

3.7. Alghero

A several-hundred-meter thick volcanic succession composed of diversely welded pyroclastic flows crops out near Alghero. The paleomagnetism of 10 flows was previously studied ([21], Table 2). Flows 1 to 6, in stratigraphic order from base to top, defines a reverse-normal-reverse polarity pattern. Although flows 7 to 10 clearly postdate flow 6, their stratigraphy is unconstrained. Lecca et al. [25] obtained an age of 20.9± 0.5 Ma (K–Ar on plagioclase) for a flow located slightly above flow 6. We studied four additional flows for paleomagnetism (LGA, LGB, LGG, LGH, Online Fig. 10), all located between flows 1 to 6 (see Table 2 for the detailed stratigraphy). Their polarities confirm the reverse-normal-reverse polarity pattern for the base of the succession. We obtained excellent, nearly identical $^{40}Ar/^{39}Ar$ incremental-heating results from two experiments from flow LGB (uppermost flow of the lower reverse-polarity interval of the succession) that yielded broad plateaus, stable Ca/K ratios, and high $\%^{40}Ar^*$ content, giving a weighted-mean isochron age of 20.71± 0.05 Ma. This suggests that flows 1 to 6 may have been emplaced during chrons 6An.2r, 6An.2n and 6An.1r, within ~500 kyr. Without additional data, we attribute the emplacement of flows 7 to 10, displaying normal and reverse polarities, to the same time interval. The succession mean inclination (Table 3) is too low by a few degrees with respect to the expected inclination. It is noteworthy that the two poorly welded flows LGB and LGH have steeper inclinations (50–55°) than the strongly welded units. This suggests that inclination

shallowing may have accompanied dense welding. Following Gattacceca and Rochette [57], we evaluated the degree of remanence anisotropy for the strongly welded flows LGA. The mean remanence anisotropy degree of 1.33 (compared to a susceptibility anisotropy degree of 1.06) accounts for an inclination shallowing of 8°. Nevertheless, as it was impossible to apply any correction to the directions obtained by De Jong et al. [21], we use in our analysis uncorrected directions, bearing in mind that the mean low inclination for the succession is an artifact due to anisotropy. The mean direction based on 14 independent directions yields a 42.1°±11.2° ccw rotation, with δ=19.5° indicating adequate averaging of secular variation.

4. Discussion

4.1. Integrity of the Corsica–Sardinia microplate (CSM)

The CSM is mainly formed by the Corsica–Sardinia batholith, a 500 km long and 50 km wide igneous structure mostly composed of Hercynian granitic rocks with remnants (mainly metamorphic rocks) of the batholith envelope [59]. This batholith was not affected by thrusting during the Alpine orogeny. Thus the post-Eocene rotations discussed here are not related to the Alpine orogeny but to the rifting and drifting event that led to the formation of the Liguro-Provençal basin.

Given the N–S elongated shape of the CSM, it is possible that the CSM did not behave as a rigid block, and one can expect a rotation gradient during the Oligo–Miocene rifting and drifting. Such a gradient from northern Corsica to southern Sardinia is indeed suggested by paleomagnetic measurements of Paleozoic rocks; post-Permian rotation estimates range from 30° in northwestern Corsica to 113° in central Sardinia ([23,60] for a review). But the age of these differential rotations is difficult to assess. The only available data, from central Sardinia, indicate 89° of rotation after the Triassic and 77° of rotation after the Jurassic (re-evaluated after [61] using updated reference poles [42]). The existence of a Tertiary rotation gradient is difficult to evaluate since most Tertiary paleomagnetic data come from central and northern Sardinia and it is difficult to find volcanic successions of the same age scattered along the CSM. We have studied three volcanic successions in the range 21–20 Ma: the southernmost one (central Sardinia) rotated slightly more than the Oniferi and Alghero areas after Aquitanian (53° instead of 42°), but this small differential rotation is not significant at the 95% confidence level. In Corsica, Miocene volcanic rocks are rare and sedimentary rocks yield ambiguous paleomagnetic results [32]. However a 35±6° post-Eocene ccw rotation for northern Corsica (re-evaluated after [32]) and a 44±4° post-Chattian ccw rotation for southern Corsica [52] have been recorded in sediments, again compatible with a rotation gradient from north to south.

The boundaries of blocks with relative rotation are difficult to locate. Paleomagnetic data from dykes crossing the straits of Bonifacio between Corsica and Sardinia indicate a 2±8° ccw rotation of Sardinia with respect to Corsica at the 95% confidence level (computed after [62]). Therefore no significant rotation took place between the two islands after the Permian. Moreover, geologic correlations [63] indicate that no significant strike-slip movement occurred in the straits of Bonifacio since the Hercynian orogeny. Therefore the possible rotations between blocks must take place along the NE-trending strike-slip faults that transect the CSM. The suggested rotation pattern is compatible with a left-lateral movement along these faults. Although the age of these faults is not precisely constrained, several workers [64–67] document that they cut Aquitanian deposits and are overlain by deposits of Burdigalian age [68].

In conclusion, it can be proposed in view of previous paleomagnetic data, that a rotation gradient occurs from north to south in the CSM. Most of these block rotations probably occurred before the Burdigalian, i.e. before the major rotation phase linked with the opening of the Liguro-Provençal oceanic basin.

4.2. Data synthesis

The Monte Torru and Monte Minerva successions are nearly coeval, encompassing the interval 18.6–19.0 Ma. They are separated by ~10 km, without significant intervening faults. Proximity in time and place allows combination of the paleomagnetic data at the single paleomagnetic direction level. The similar age obtained for the Osilo andesites (18.90±0.07 Ma) suggests that we can also combine the paleomagnetic directions from this area if we exclude the possibility of significant Burdigalian differential block rotations. After combining these three volcanic successions, two directions from the Osilo succession are rejected by Vandamme's criteria [40]. The 15 independent paleomagnetic directions define a 20.8±7.8° rotation that may be regarded as the best available estimate of Sardinia ccw rotation after 18.8 Ma, even if secular variation may not have been entirely accommodated (δ=12.4°). Similarly, directions from Central Sardinia, Oniferi and Alghero can be combined (at the single paleomagnetic direction level) since they belong to the same time interval (20.9–

20.2 Ma). The 35 independent directions define a 45.9± 8.6° rotation (δ=21.1°) that may be regarded as the best available estimate of Sardinia ccw rotation after 20.5 Ma. Inversion tests cannot be performed on these data, as variable and unknown inclination shallowing correction would have to be performed on the data from Alghero (see discussion in Section 3.7). It is noteworthy that in the first case (Monte Minerva, Monte Torru, Osilo), the rotation estimates obtained from each succession alone (Table 3) are not compatible and sometimes significantly different from the rotation estimated from the combined successions. This is attributed to the low scatter of the paleomagnetic directions in each succession and the limited number of independent directions. In the second case (central Sardinia, Oniferi, Alghero), the three estimates are compatible and close to the rotation estimated from the combined successions. In this case, the scatter in each succession is sufficient to provide a reliable estimate of the rotation angle. This clearly illustrates the fact that the bias introduced by secular variation, if not properly taken into account, can lead to rotation estimates that are incorrect by tens of degrees in our case: 35° for Monte Torru, 12° for Monte Minerva, −4° for Osilo, compared to 21° when combining the three successions (Table 3). This is why pre-existing data could not be used to precisely constrain the rotation history of the CSM, since they were neither acquired in a detailed stratigraphic framework, nor dated with sufficient precision.

The new results define a coherent evolution of the Sardinian rotation angle (Fig. 7), suggesting that secular variation was sufficiently averaged. The reliability of our mean paleomagnetic directions is also supported by agreement in inclination with that expected for Early Miocene, as indicated by the absence of significant flattening. Only two instances from Sardinian sediments (sites M and L of [29]) lie off the proposed rotational trend. We tentatively ascribe this discrepancy to poor geochronological constraints or remagnetization.

4.3. Kinematic and geodynamic implications

The paleomagnetic and geochronological data of the central Sardinia, Alghero, and Oniferi areas indicate a ccw rotation of ~45° after ~20.5 Ma. This angle can be regarded as the minimum rotation occurring during the CSM drift, since an additional rotation may have taken place between the end of rifting (~21.5 Ma) and 20.5 Ma. This is a marked increase over the previous estimate of 30° [26]. We believe the explanation for this discrepancy lies in the lack of precise stratigraphic and geochronological control obtained during previous studies. Three volcanic successions (Osilo andesites,

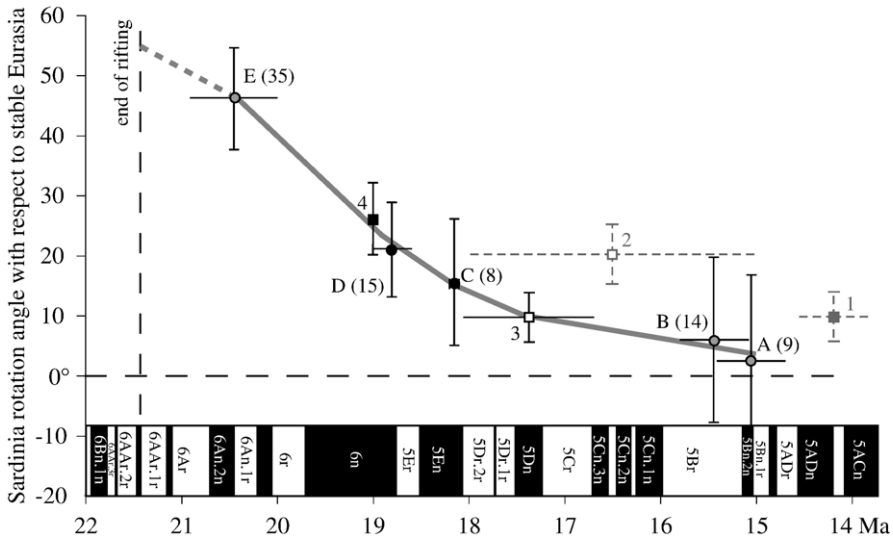

Fig. 7. Rotation angle of Sardinia with respect to stable Europe versus time. Circles represent the results from one or a group of volcanic successions with indication of the paleomagnetic polarity (solid circle: normal polarity; empty circle: reverse polarity; shaded circle: both reverse and normal polarities). The number of independent paleomagnetic directions is given in parentheses. The horizontal "error bars" indicate the time span covered by the volcanic successions rather than geochronological uncertainties. A: Terminal andesites, B: Sulcis, C: Monte Furru [27], D: Monte Minerva/Monte Torru/Osilo, E: Central Sardinia/Alghero/Oniferi. Boxes are results from sediments from the Marmilla area (1, 2, 3: [29]; 4: [30]) with indication of polarity. Magnetostratigraphic scale is from [45]. The 55° rotation angle at the end of rifting is deduced from the post-rift reconstruction by Gueguen [7] ('model A' of Fig. 2).

Monte Minerva, Monte Torru) provide well-constrained tie-points demonstrating that 21° of rotation occurred after 18.8 Ma. This result is in agreement with that obtained by Speranza et al. [30] from Sardinian sedimentary rocks, indicating a post 19 Ma 25.8±5.9° rotation (recomputed using the 20 Ma Eurasian paleomagnetic pole from [42]). As evidenced in Edel et al. [31], the timing of the termination of the rotation is difficult to assess precisely because: (1) rotations of less than about 5° are hard to prove on the basis of paleomagnetic evidence, (2) data are scarce for the 18–16 Ma interval, and (3) rotation may slow asymptotically, making an 'end point' hard to define. Nevertheless, our results from the terminal andesites and Sulcis suggest that the rotation is virtually complete by 15 Ma.

These conclusions are compatible only with 'Model A' of Fig. 2, i.e. the pre-drift palinspastic reconstruction deduced from morphological fit of the continental margins, that implies a Miocene ccw rotation of about 55° after the end of rifting (~21.5 Ma). If we accept this pre-drift reconstruction, our data indicate that about 10° of ccw rotation must occur between ~21.5 Ma and 20.5 Ma. This reconstruction is compatible with geological correlations between Sardinia–Corsica and Provence [1]. It also agrees with oceanic crust extension defined by tectonic subsidence analysis [14] and compatible with the constraints on Moho depth obtained from 3D gravity inversion [69]. The total amount of opening of the southern part of the basin is ~400 km during the drift. Between 20.5 and 18 Ma, with a rotation pole located in the Ligurian Sea around 43.5°N, 9.5°E, the average rate for the opening of the basin reaches 9 cm yr^{-1} for the southern part of the basin.

According to paleomagnetic data, the Adriatic/Ionian lithosphere has been rigidly attached to Africa since the Late Cretaceous (e.g. [70–73]). It has thus moved northward at a rate of 6–7 mm yr^{-1} with respect to Europe during the Miocene (e.g. [74]). Prior to the rotation of Corsica and Sardinia in the Miocene there was a very slow oblique convergence between the CSM and Adria, and no convergence at all after 16–15 Ma since the Adria displacement parallels the CSM microplate border. In this slow convergence setting, the occurrence of velocities up to 9 cm yr^{-1} during the apex of the opening could be explained by the dynamics of the Adriatic/Ionian slab roll-back [3,75]. Remarkably high opening rates have also been evidenced for the Plio–Pleistocene opening of the southern Tyrrhenian oceanic basin [76] that is also related to the Adriatic/Ionian slab roll-back.

The proposed reconstruction ('Model A') indicates the existence of a lowermost Miocene continuous calc-alkaline volcanic arc more than 1000 km long encompassing the Valencia Trough volcanism [13], the lower part of Sardinian rift volcanism (Fig. 5), its submarine prolongation to the SW of Corsica [77], the few remnants in SE Corsica [33], and remnants of volcanic activity in Provence (e.g. at Villeneuve-Loubet, Antibes, Cap d'Ail, Biot). This volcanic arc is linked to the subduction of Adriatic/Ionian oceanic crust beneath Sardinia and Corsica [28].

5. Conclusions

While available paleomagnetic data from Sardinian Miocene volcanic rocks could not be properly interpreted because of the lack of a sufficient chronostratigraphic framework, new paleomagnetic data interpreted in the light of $^{40}Ar/^{39}Ar$ incremental-heating ages and detailed field studies permit a kinematic reconstruction for Sardinia rotation and associated Liguro-Provençal basin opening. Whereas previously published results documented only 30° of ccw rotation during the Miocene drift, we present conclusive and well-dated evidence for a much higher rotation. Sardinia rotated ccw 45° with respect to stable Europe between 20.5 and 15 Ma. Movement is most rapid during the period 20.5–18 Ma when 30° of rotation occurred. This interval of fastest rotation is also approximately the time of greatest volcanism. The Sardinian rotation is complete at 15 Ma. This post-rifting minimum 45° rotation angle is compatible only with palinspastic reconstruction locating the CSM near the European margin. This reconstruction implies a broad oceanic domain in the Liguro-Provençal basin (up to 400 km in the southern part) and high drift rate between 20.5 and 18 Ma (up to 9 cm yr^{-1} for the southern part). In the overall context of the Africa–Eurasia slow convergence, such high rates and large extent of oceanic spreading are likely the consequence of Adriatic/Ionian slab roll-back towards the E–SE.

Acknowledgements

We acknowledge careful and constructive reviews by Cor Langereis and an anonymous reviewer, as well as constructive comments by Fabio Speranza on an earlier version. We thank A. Assorgia, C. Coulon, A. Demant and G. Oggiano for useful discussion about the geology of Sardinia. G. Oggiano is also acknowledged for field trips in the Anglona area. We are grateful to J.-J. Lamora for his invaluable help on the field. Most of this work was funded by a Ph.D. grant from the Ecole des Mines de Paris, France (JG).

Appendix A. Supplementary data

Supplementary data associated with this article can be found, in the online version, at doi:10.1016/j.epsl.2007.02.003.

References

[1] M. Westphal, J.B. Orsini, P. Vellutini, Le microcontinent corso-sarde, sa position initiale: données paléomagnétiques et raccords géologiques, Tectonophys. 30 (1976) 141–157.

[2] E. Gueguen, C. Doglioni, M. Fernandez, On the post-25 Ma geodynamic evolution of the Western Mediterranean, Tectonophys. 298 (1998) 259–269.

[3] C. Faccenna, M. Mattei, R. Funiciello, L. Jolivet, Styles of back-arc extension in the Central Mediterranean, Terra Nova 9 (1997) 126–130.

[4] R. Vially, P. Trémolières, Geodynamics of the Gulf of Lions: implications for petroleum exploration, in: P.A. Ziegler, F. Horvàth (Eds.), Peri-Tethys Memoir 2: Structure and Prospects of Alpine Basins and Forelands, Mém. Muséum national d'Histoire naturelle, vol. 170, 1996, pp. 129–158.

[5] M. Westphal, C. Bardon, A. Bossert, R. Hamzeh, A computer fit for Corsica and Sardinia against Southern France, Earth Planet. Sci. Lett. 18 (1973) 137–140.

[6] J.P. Réhault, Evolution tectonique et sédimentaire du bassin ligure (Méditerranée occidentale), Ph.D. Thesis, Univ. Paris VI (France), 1981.

[7] E. Gueguen, Le bassin Liguro-Provençal: un véritable océan, Ph. D. Thesis, Université de Bretagne Occidentale, Brest (France), 1995.

[8] J. Burrus, Contribution to a geodynamic synthesis of the Provençal basin (north-western Mediterranean), Mar. Geol. 55 (1984) 247–269.

[9] J.B. Edel, Etude paléomagnétique en Sardaigne. Conséquences pour la géodynamique de la Méditerannée occidentale, Ph.D. Thesis, Institut de Physique du Globe, Université Louis Pasteur, Strasbourg (France), 1980.

[10] J.P. Réhault, N. Bethoux, Earthquake relocation in the Ligurian sea (Western Mediterranean): geological interpretation, Mar. Geol. 55 (1984) 429–445.

[11] S. Le Douaran, J. Burrus, F. Avedik, Deep structure of the North-Western Mediterranean basin: result of a two-ship seismic survey, Mar. Geol. 55 (1984) 325–345.

[12] G.P. Pascal, A. Mauffret, P. Patriat, The ocean–continent boundary in the Gulf of Lion from analysis of expanding spread profiles and gravity modelling, Geophys. J. Int. 113 (1993) 701–726.

[13] A. Mauffret, G. Pascal, A. Maillard, C. Gorini, Tectonics and deep structure of the northwestern Mediterranean basin, Mar. Pet. Geol. 12 (1995) 645–666.

[14] V. Pasquale, M. Verdoya, P. Chiozzi, Rifting and thermal evolution of the Northwestern Mediterranean, Ann. Geofis. 38 (1995) 43–53.

[15] I. Contrucci I., Structures profondes du bassin Nord Ligure et structures du bassin Nord Tyrrhénien, Ph.D. thesis, Université de Corse, France, 1999.

[16] A. Galdeano, J.C. Rossignol, Assemblage à altitude constante des cartes d'anomalies magnétiques couvrant l'ensemble du bassin occidental de la Méditerranée, Bul. Soc. Géol. France 19 (1977) 461–468.

[17] J. Cravatte, P. Dufaure, M. Prim, S. Rouaix, Les forages du golfe du Lion, stratigraphie, sédimentologie, Compagnie française des pétroles, Notes Mém. 11 (1974) 209–274.

[18] A. Cherchi, L. Montadert, Oligo–Miocene rift of Sardinia and the early history of the Western Mediterranean Basin, Nature 298 (1982) 736–739.

[19] M. Seranne, The Gulf of Lion continental margin (NW Mediterranean) revisited by IBS: an overview, in: B. Durand, A. Mascle, L. Jolivet, F. Horvàth, M. Séranne (Eds.), The Mediterranean basins: tertiary extension within the Alpine orogen, Geol. Soc. London, Spec. Publ., vol. 156, 1999, pp. 21–53.

[20] C. Gorini, A. Le Marrec, A. Mauffret, Contribution to the structural and sedimentary history of the gulf of Lions (western Mediterranean), from the ECORS profiles, industrial seismic profiles and well data, Bull. Soc. Géol. Fr. 164 (1993) 353–363.

[21] K.A. De Jong, M. Manzoni, J.D.A. Zijderveld, Paleomagnetism of the Alghero trachyandesites, Nature 244 (1969) 67–69.

[22] M. Todesco, L. Vigliotti, When did Sardinia rotated? Statistical evaluation of paleomagnetic data, Ann. Geofis. 36 (1993) 119–134.

[23] F. Speranza, Paleomagnetism and the Corsica–Sardinia rotation: a short review, Boll. Soc. Geol. Ital. 118 (1999) 537–543.

[24] L. Beccaluva, L. Civetta, G. Macciota, C.A. Ricci, Geochronology in Sardinia: results and problems, Rend. Soc. Ital. Mineral. Petrol. 40 (1985) 57–72.

[25] L. Lecca, R. Lonis, S. Luxoro, E. Melis, F. Secchi, P. Brotzu, Oligo–Miocene volcanic sequences and rifting stages in Sardinia: a review, Per. Mineral. 66 (1997) 7–61.

[26] R. Montigny, J.B. Edel, R. Thuizat, Oligo–Miocene rotation of Sardinia: K/Ar ages and paleomagnetic data of Tertiary volcanics, Earth Planet. Sci. Lett. 54 (1981) 262–271.

[27] A. Deino, J. Gattacceca, R. Rizzo, A. Montanari, $^{40}Ar/^{39}Ar$ dating and paleomagnetism of the Miocene volcanic succession of Monte Furru (western Sardinia): implications for rotation history the Corsica–Sardinia microplate, Geophys. Res. Lett. 28 (2001) 3373–3376.

[28] C. Coulon, Le volcanisme calco-alcalin cénozoïque de Sardaigne (Italie) pétrographique, géochimie et genèse des laves andésitiques et des ignimbrites, signification géodynamique, Ph.D. Thesis, Université d'Aix-Marseille (France), 1977.

[29] L. Vigliotti, V.E. Langenheim, When did Sardinia stop rotating? New paleomagnetic results, Terra Nova 7 (1995) 424–435.

[30] F. Speranza, I.M. Villa, L. Sagnotti, F. Florindo, D. Cosentino, P. Cipollari, M. Mattei, Age of the Corsica–Sardinia rotation and Liguro-Provençal spreading: new paleomagnetic and Ar/Ar evidence, Tectonophys. 347 (2002) 231–251.

[31] J.-B. Edel, D. Dubois, R. Marchant, J. Hernandez, M. Cosca, La rotation miocène inférieur du bloc corso-sarde. Nouvelles contraintes paléomagnétiques sur la fin du mouvement, Bull. Soc. Géol. Fr. 172 (2001) 275–283.

[32] L. Vigliotti, D.V. Kent, Paleomagnetic results of Tertiary sediments from Corsica: evidence of post-Eocene rotation, Phys. Earth Planet. Inter. 62 (1990) 97–108.

[33] J. Ferrandini, J. Gattacceca, M. Ferrandini, A. Deino, M.C. Janin, Chronostratigraphy and paleomagnetism of Oligo–Miocene deposits of Corsica (France): geodynamic implications for the Liguro-Provençal basin spreading, Bull. Soc. Géol. Fr. 174 (2003) 357–371.

[34] M. Alexandrescu, V. Courtillot, J.-L. Le Mouël, High-resolution secular variation of the geomagnetic field in western Europe over the last 4 centuries: comparison and integration of historical data from Paris and London, J. Geophys. Res. 102 (1997) 20245–20258.

[35] J.C. Tanguy, M. Le Goff, V. Chillemi, A. Paiotti, C. Principe, S. La Delfa, G. Patané, Variation séculaire de la direction du champ

géomagnétique enregistrée par les laves de l'Etna et du Vésuve pendant les deux derniers millénaires, C. R. Acad. Sci. Paris 329 (1999) 557–564.
[36] P.R. Renne, C.C. Wisher, A.L. Deino, D.B. Karner, T.L. Owens, D.J. De Paolo, Intercalibration of standards, absolute ages and uncertainties in $^{40}Ar/^{39}Ar$ dating, Chem. Geol. 145 (1998) 117–152.
[37] J.L. Kirschvink, The least-square line and plane and the analysis of paleomagnetic data, Geophys. J. R. Astron. Soc. 62 (1980) 699–718.
[38] R. Fisher, Dispersion on a sphere, Proc. R. Soc. Lond., A 217 (1953) 295–305.
[39] J.P. Cogné, PaleoMac: a Macintosh™ application for treating paleomagnetic data and making plate reconstructions, Geochem. Geophys. Geosyst. 4 (2003), doi:10.1029/2001GC000227.
[40] D. Vandamme, A new method to estimate paleosecular variation, Phys. Earth Planet. Inter. 85 (1994) 131–142.
[41] M.W. McElhinny, P.L. McFadden, R.T. Merrill, The myth of the Pacific dipole window, Earth Planet. Sci. Lett. 143 (1996) 13–22.
[42] J. Besse, V. Courtillot, Apparent and true polar wander and the geometry of the geomagnetic field in the last 200 million years, J. Geophys. Res. 107 (2002), doi:10.1029/2000JB000050.
[43] H.H. Demarest, Error analysis for the determination of tectonic rotation from paleomagnetic data, J. Geophys. Res. 88 (1983) 4321–4328.
[44] M.W. McElhinny, P. McFadden, Paleosecular variation over the past 5 Myr based on a new generalized database, Geophys. J. Int. 131 (1997) 240–252.
[45] L. Lourens, F. Hilgen, N.J. Shackleton, J. Laskar, D. Wilson, in: F.M. Gradstein, J.G. Ogg, A.G. Smith (Eds.), The Neogen period, in a Geologic Time Scale 2004, Cambridge University Press, 2004, pp. 409–440.
[46] A. Demant, Contribution à l'étude du volcanisme tertiaire de la Sardaigne nord-occidentale; Le cycle andésitique terminal, Ph.D. Thesis, Université de Provence, Marseille (France), 1972.
[47] C. Coulon, A. Demant, H. Bellon, Premières datations par la méthode K/Ar de quelques laves cénozoïques et quaternaires de Sardaigne nord-occidentale, Tectonophys. 22 (1974) 41–57.
[48] C. Bobier, C. Coulon, Résultats préliminaires d'une étude paléomagnétique des formations volcaniques tertiaires et quaternaires du Logudoro (Sardaigne septentrionale), C. R. Acad. Sci. Paris 270 (1970) 1434–1437.
[49] C. Coulon, A. Demant, C. Bobier, Contribution du paléomagnétisme à l'étude des séries volcaniques cénozoïques et quaternaires deSardaigne nord-occidentale, Tectonophys. 22 (1974) 59–82.
[50] M. Manzoni, A. Ferriani, Trattamento statistico e validità dei dati paleomagnetici delle vulcaniti terziarie della Sardegna, Boll. Soc. Geol. Ital. 95 (1976) 1263–1281.
[51] M. Manzoni, A. Marini, L. Vigliotti, Dislocazioni tettoniche dedotte dalle direzioni di magnetizzazione primaria del distretto vulcanico di Sarroch (Sardegna), Boll. Geofis. Teor. Appl. 22 (1980) 139–152.
[52] A. Assorgia, A. Fadda, G. Gimeno Torrente, V. Morra, L. Ottelli, F.A. Secchi, Le successioni ignimbritiche terziarie del Sulcis (Sardegna sud-occidentale), Mem. Soc. Geol. Ital. 45 (1990) 951–963.
[53] C. Garbarino, L. Lirer, L. Maccioni, I. Salvadori, Carta vulcanologica della'Isola di San Pietro (Sardegna). Scala 1/25000, SELCA Eds, Firenze (Italy), 1990.
[54] S. Pasci, L. Pioli, G. Pisanu, M. Rosi, V. Sale, E. Benvenuti, M. Laurenzi, Tettonica e vulcanismo miocenici nel Sulcis (Sardegna SW), Abstract *in* Geoitalia, III FIST meeting, 5–8 September 2001, Chieti (Italy), 2001.
[55] V. Morra, F.A. Secchi, A. Assorgia, Petrogenesic significance of peralkaline rocks from Cenozoic calc-alkaline volcanism from SW Sardinia, Italy, Chem. Geol. 118 (1994) 109–142.
[56] M. Manzoni, Un'interpretazione dei dati paleomagnetici del Terziario della Sardegna ed alcuni nuovi risultati, Rend. Semin. Fac. Sci. Univ. Cagliari (1974) 283–295.
[57] J. Gattacceca, P. Rochette, Pseudopaleosecular variation due to remanence anisotropy in a pyroclastic flow succession, Geophys. Res. Lett. 29 (2002), doi:10.1029/2002GL014697.
[58] A. Assorgia, S. Barca, A. Porcu, C. Spano, K. Balogh, R. Rizzo, The Oligocene–Miocene sedimentary and volcanic successions of central Sardinia, Italy, Rom. J. Stratigr. 78 (1998) 9–23.
[59] P. Rossi, Organisation et genèse d'un grand batholite orogénique: le batholite calco-alcalin de la Corse. Ph.D. Thesis, University Toulouse (France), 1986.
[60] J.B. Edel, Hypothèse d'une ample rotation horaire tardi-varisque du bloc Maures-Estérel-Corse-Sardaigne, Géol. Fr. 1 (2000) 3–19.
[61] F. Horner, W. Lowrie, Paleomagnetic evidence from Mesozoic carbonate rocks for the rotation of Sardinia, J. Geophys. 49 (1981) 11–19.
[62] L. Vigliotti, W. Alvarez, M. McWilliams, No relative rotation detected between Corsica and Sardinia, Earth Planet. Sci. Lett. 98 (1990) 313–318.
[63] F. Arthaud, P. Matte, Détermination de la position initiale de la Corse et de la Sardaigne à la fin de l'orogenèse hercynienne grâce aux marqueurs géologiques anté-mésozoïques, Bull. Soc. Géol. Fr. 19 (1977) 833–840.
[64] A. Funedda, G. Oggiano, S. Pasci, The Logudoro basin: a key area for the tertiary tectono-sedimentary evolution of North Sardinia, Boll. Soc. Geol. Ital. 119 (2000) 31–38.
[65] G. Oggiano, S. Pasci, A. Funedda, Il Bacino di Chilivani-Berchidda: un esempio di struttura transtensiva. Possibili relazioni con la geodinamica Cenozoica del Mediterraneo Occidentale, Boll. Soc. Geol. Ital. 114 (1995) 465–475.
[66] L. Carmignani, S. Barca, L. Disperati, P. Fantozzi, A. Funedda, G. Oggiano, S. Pasci, Tertiary compression and extension in the Sardinian basement, Boll. Geofis. Teor. Appl. 36 (1994) 141–144.
[67] L. Carmignani, F.A. Decandia, L. Disperati, P. Fantozzi, A. Lazzarotto, D. Liotta, G. Oggiano, Relationships between the tertiary structural evolution of the Sardinia–Corsica–Provençal domain and the northern Apennines, Terra Nova 7 (1995) 128–137.
[68] S. Pasci, Tertiary transcurrent tectonics of North-Central Sardinia, Bull. Soc. Géol. Fr. 168 (1997) 301–312.
[69] N. Chamot-Rooke, J.-M. Gaulier, F. Jestin, Constraints on Moho depth and crustal thickness in the Liguro-Provençal basin from a 3D gravity inversion: geodynamic implications, in: B. Durand, L. Jolivet, F. Horvath, M. Seranne (Eds.), The Mediterranean Basins: Tertiary Extension Within the Alpine Orogen, Geol. Soc. London, Spec. Publ., vol. 156, 1999, pp. 37–61.
[70] J.E.T. Channell, D.H. Tarling, Paleomagnetism and the rotation of Italy, Earth Planet. Sci. Lett. 25 (1975) 177–188.
[71] J.E.T. Channell, Paleomagnetic data from Umbria (Italy): implication for the rotation of Adria and Mesozoic apparent polar wander paths, Tectonophys. 216 (1992) 365–378.
[72] R. Van der Voo, Paleomagnetism of the Atlantic, Tethys and Iapetus Oceans, Cambridge University Press, Cambridge, 1993, 411 pp.
[73] G. Muttoni, E. Garzanti, L. Alfonsi, S. Cirilli, D. Germani, W. Lowrie, Motion of Africa and Adria since the Permian: paleomagnetic and paleoclimatic constraints from northern Libya, Earth Planet. Sci. Lett. 192 (2001).

[74] L.A. Savostin, J.C. Sibuet, L.P. Zonenshain, X. Le Pichon, J.M. Roulet, Kinematic evolution of the Tethys belt from the Atlantic Ocean to the Pamirs since the Triassic, Tectonophysics 123 (1986) 1–35.
[75] A. Malinverno, W.B.F. Ryan, Extension in the Tyrrhenian sea and shortening in the Apennines as a result of arc migration driven by sinking of the lithosphere, Tectonics 5 (1986) 227–245.
[76] I. Nicolosi, F. Speranza, M. Chiappini, Ultrafast oceanic spreading of the Marsili Basin, southern Tyrrhenian Sea: evidence from magnetic anomaly analysis, Geology 34 (2006) 717–720.
[77] P. Rossi, P. Guennoc, J.P. Réhault, N. Arnaud, B. Jakni, G. Poupeau, M. Tegyey, J. Ferrandini, M. Sosson, M.O. Beslier, N. Rolet, R. Gloguen, Importance du volcanisme calco-alcalin miocène sur la marge sud-ouest de la Corse (campagne MARCO), C. R. Acad. Sci. Paris 327 (1998) 369–376.
[78] A. Cox, Confidence limits for the precision parameter k, Geophys. J. R. Astron. Soc. 18 (1969) 545–549.
[79] L. Pioli, M. Rosi, Rheomorphic structures in a high-grade ignimbrite: the Nuraxi tuff, Sulcis volcanic district (SW Sardinia, Italy), J. Volcanol. Geotherm. Res. 142 (2005) 11–28.